Capturing Interactions between Nitrogen and Hydrological Cycles under Historical Climate and Land Use: Susquehanna Watershed Analysis with the GFDL Land Model LM3-TAN

M. Lee[1], S. Malyshev[2], E. Shevliakova[2], P. C. D. Milly[3], and P. R. Jaffé[1]

[1]{Department of Civil and Environmental Engineering, Princeton University, Princeton, NJ, USA}

[2]{NOAA/Geophysical Fluid Dynamics Laboratory - Princeton University Cooperative Institute for Climate Science, Princeton, NJ, USA}

[3]{U. S. Geological Survey and NOAA/Geophysical Fluid Dynamics Laboratory, Princeton, NJ, USA}

Correspondence to: M. Lee (minjinl@princeton.edu)

Abstract

We developed a process model LM3-TAN to assess the combined effects of direct human influences and climate change on Terrestrial and Aquatic Nitrogen (TAN) cycling. The model was developed by expanding NOAA's Geophysical Fluid Dynamics Laboratory land model LM3V-N of coupled terrestrial carbon and nitrogen (C-N) cycling and including new N cycling processes and inputs such as a soil denitrification, point N sources to streams (i.e. sewage), and stream transport and microbial processes. Because the model integrates ecological, hydrological, and biogeochemical processes, it captures key controls of transport and fate of N in the vegetation-soil-river system in a comprehensive and consistent framework which is responsive to climatic variations and land use changes. We applied the model at 1/8 degree resolution for a study of the Susquehanna River basin. We simulated with LM3-TAN stream dissolved organic-N, ammonium-N, and nitrate-N loads throughout the river network, and we evaluated the modeled loads for 1986-2005 using data from 16

monitoring stations as well as a reported budget for the entire basin. By accounting for inter-annual hydrologic variability, the model was able to capture inter-annual variations of stream N loadings. While the model was calibrated with the stream N loads only at the last downstream Susquehanna River Basin Commission station Marietta (40.02' N, 76.32' W), it captured the N loads well at multiple locations within the basin with different climate regimes, land use types, and associated N sources and transformations in the sub-basins. Furthermore, the calculated and previously reported N budgets agreed well at the level of the whole Susquehanna watershed. Here we illustrate how point and non-point N sources contributing to the various ecosystems are stored, lost, and exported via the river. Local analysis for 6 sub-basins showed combined effects of land use and climate on soil denitrification rates, with the highest rates in the Lower Susquehanna Sub-basin (extensive agriculture; Atlantic coastal climate) and the lowest rates in the West Branch Susquehanna Sub-basin (mostly forest; Great Lakes and Midwest climate). In the re-growing secondary forests, most of the N from non-point sources was stored in the vegetation and soil, but in the agricultural lands most N inputs were removed by soil denitrification indicating that anthropogenic N applications could drive substantial increase of N_2O emission, an intermediate of the denitrification process.

1 Introduction

Biologically available nitrogen (N) in terrestrial ecosystems has significantly increased via anthropogenic nutrient inputs: artificial fertilizer, cultivation of N fixing crops, and fossil fuel consumption (Galloway et al., 2004; 2008). This increase has caused acidification and N saturation in some terrestrial and aquatic ecosystems (Henriksen and Brakke, 1988; Kelly et al., 1990; Murdoch and Stoddard, 1992; Howarth, 2002). N-saturated soils and streams are also major sources of nitrous oxide (N_2O) emissions, which is a potent greenhouse gas (Albritton et al., 1994). Other concerns include severe water-quality problems associated with cultural eutrophication, which results in harmful algal blooms and hypoxia in rivers, lakes, estuaries, and coastal zone ecosystems (Smith, 2003; Smith et al., 2006). Climate change and variability also affect water quality through the distribution of high and low flow extremes (Scavia et al., 2002; Howarth et al., 2006). It is generally accepted that microbial processes related to the N cycle are strongly influenced by abiotic factors, and warm or wet climate

provides favorable environments for certain groups of bacterial activities. Quantification and management of the diverse and coupled effects of human activity and climate change on N cycling requires a comprehensive model of the relevant coupled processes that can support the design of optimal nutrient loading controls to maintain desirable water quality and terrestrial ecosystem integrity.

To characterize implications of human and climate driven perturbation in the earth N cycling and its implication for water and air quality, the next-generation of N cycling models need to (1) account for regional and local changes in terrestrial and aquatic ecosystem structure and functioning, (2) represent in a consistent manner emissions and transformation of N to air, rivers and coasts, and (3) be global in extent and integrated with climate and earth system models. Previously, none of the existing models addressed the above 3 challenges. Here we present a novel modeling framework capable of addressing these challenges and, prior to its global application, we evaluate this modeling framework in the Susquehanna River Basin whose sub-basins vary in climate, land use, and associated N sources and transformations, with the detailed dataset of observations.

There has been keen interest and progress in modeling the N cycle in terrestrial ecosystems. However, in most models vegetation and land use type distribution are prescribed and do not change in time. Modeling studies with EPIC, ANIMO, and CENTURY/DAYCENT typically prescribe crop distribution and simulate crop production and related nutrient and carbon (C) cycling (Sharpley and Williams, 1990; Parton et al., 1993; Williams et al., 1995; Kroes and Roelsma, 1998; Del Grosso et al., 2009). Because these models do not simulate decadal-to-century changes in vegetation structure (e.g. forest regrowth after harvesting) they are likely to overlook changes in the storage of N in vegetation. Furthermore, during wood harvesting and forest clearing for agriculture, biomass residue is an important additional input to the soil organic C-N pools. Such additional N inputs lead to additional N inorganic loads. In addition, many regional models (e.g. EPIC, ANIMO), which have been applied to far smaller basins compared to the Susquehanna watershed, often use basin-specific parameters for mineralization, nitrification, and denitrification, which complicates their application on a global scale for decadal-to-century scale studies. LM3-TAN is capable of describing N dynamics with a universal parameter set – the same parameters for all of the sub-basins within

an area of 71,220 km^2 and time periods for this simulation. LM3-TAN is among very few modeling frameworks (e.g. CLM-CN: Thornton et al 2007; CLM4MOD: Thomas et al., 2013) that can be used as a component of an ESM – that is it is capable to represent sub-diurnal exchanges of moisture, energy, C and N species among land-atmosphere. Unlike CLM4MOD, LM3-TAN simulates water quality in the rivers and nutrient loadings to the coastal environment.

Contrary to the simulations of land models limited to the terrestrial component, most watershed models do estimate stream N concentrations and loads, but they simplify or neglect many key mechanisms describing terrestrial N dynamics (e.g., vegetation and land-use dynamics, interactive C-N feedbacks on vegetation and soil microbial processes; phenological leaf drop and its contribution to soil organic matter pools). INCA-N and SWAT are widely used Geographic Information System-based watershed models (Wade et al., 2002; Schilling and Wolter, 2009). However, when it comes to large scale applications, because these models are semi-distributed, they are less capable of representing spatial variability, requiring users to define the number and sizes of sub-basins, in which land use and all of the processes for each land use are assumed to be homogeneous and needed to be defined individually. This limits their ability to analyze complex land-use management scenarios. In this class of models, RHESSys is one of a few models with an ecology component that can be used to investigate interactions between ecosystems and hydrological processes according to climate variability (Tague and Band, 2004; Beckers et al., 2009). However, like most models, because these models do not simulate vegetation and land use type distribution, a specific parameter set that describes typical soil, vegetation, and land use characteristics has to be developed using its special module when a study site requires different vegetation or soil types from its default application. This explains why RHESSys has only been applied to very small or sub sections of catchments (Band et al., 2001; Tague and Band, 2004).

Given the current lack of models that link terrestrial C-N cycling, long-term vegetation and land-use dynamics to N loads and concentrations in streams, accounting for different N species, the goal of this research was to build a model to simulate stream N loads that is based on a global-scale terrestrial and N-enabled land model, followed by its testing on a large and

complex watershed, for which many years of stream discharge and stream N data are available. For this purpose and to assess the combined effects of direct human influences and climate change on Terrestrial and Aquatic Nitrogen (TAN) cycling, we developed a process model LM3-TAN. The new features include integrated effects of point and non-point sources on river N loads, a soil denitrification module, and stream microbial processes.

We applied LM3-TAN to the Susquehanna River basin, the largest of the watersheds in the northeastern U.S., draining an area of 71,220 square kilometers, at the resolution of 1/8 degree. The model was evaluated using 20 year (1986-2005) data of stream ammonium (NH_4^+) and dissolved organic N loads as well as stream nitrate (NO_3^-) N loads from 16 monitoring stations. For each of 6 sub-basins, we conducted local analysis to assess combined effects of land use and climate on the soil denitrification. We then built up a N budget and compared it with the corresponding reported budget to better understand how point and non-point N sources contributing to the various ecosystems are stored, lost, and exported via the river at the level of the whole Susquehanna watershed. Although there are several parameters that required calibration by fitting simulated to reported stream N loads, these parameters are used universally for the entire basin where climate, soil, vegetation, and land use characteristics vary. Efforts have been made in the development of this model to limit the number of calibrated parameters.

2 Model Description

2.1 Overview

LM3V-TAN is an expansion of earlier GFDL land models, beginning with LM3V of Shevliakova et al (2009), which describes vegetation and C dynamics. LM3-TAN was expanded to include vegetation- and soil-N dynamics from LM3V-N (Gerber et al., 2010), new soil physics and hydrology from LM3 (Milly et al, 2014), and N cycling processes described here. LM3 was used as a component of the GFDL Earth System Models (Dunne et al, 2012) and included several enhancements, such as vertically resolved soil physics and hydrology and explicit river dynamics and physics. LM3-TAN includes soil denitrification and transport and chemistry of N cycle in rivers. This version of model allows more complete

tracking of N through the soil-river continuum. In this section, we first summarize key features of the model, and then we describe the newest N cycling features.

LM3V simulates distribution of five vegetation functional types (C3 and C4 grasses, and temperate-deciduous, tropical, and cold-evergreen trees) on the basis of total biomass and prevailing climate conditions. The model tracks hundreds of years of land use change using global land use transition scenarios that were historically reconstructed by combining satellite-based contemporary patterns of agriculture with historical data on agriculture and population (Hurtt et al., 2006). The four land use types are natural vegetation (land undisturbed by human activities), secondary vegetation (land formerly disturbed by human activities), cropland, and pasture. The model is spatially distributed, and each grid cell consists of up to 15 tiles: 1 natural vegetation, 1 cropland, 1 pasture, and 1 to 12 secondary vegetation tiles representing unique disturbance histories (i.e. de/reforestation, agricultural practice change). Exchanges of water, energy, and between land and atmosphere are computed with a time step of 30 minutes. Atmospheric and terrestrial reservoirs include C pools in vegetation (leaves, fine roots, sapwood, heartwood, and labile C storage), soil (fast and slow), and anthropogenic storage. The C pools in the vegetation are updated on a daily time step to account for vegetation growth and allocation, leaf drop and display, and natural mortality and fire. The soil C, which is supplied by the vegetation both naturally and during land-use conversion, is stored in two pools with different turnover times.

2.2 Coupled C-N dynamics in vegetation and soil

The previous two soil C pools in LM3V were divided into four pools (fast and slow litter, and slow and passive soil organic matter) in LM3V-N. Each C pool in the vegetation and soil was paired with a respective N compartment using pool-specific C:N ratios. The decomposition processes release biologically available forms of N ($NO_3^- - N$; $NH_4^+ - N$). This allows to simulate N limitation on plant growth and biological N fixation as well as N feedbacks on organic matter decomposition and stabilization. Inorganic N is removed by sorption to soil particles, plant uptake, immobilization into long-lived organic compounds, and hydrological leaching, while organic N is lost through fire, hydrological leaching, and mineralization. Loss

of nitrate N by soil denitrification was not differentiated from the hydrological nitrate-N leaching in LM3V-N.

2.3 Improved soil and river physics and hydrology

LM3 introduced vertically distributed soil-water, soil-ice and temperature profiles extending many meters below the surface, but with high resolution (thinnest layer 0.02 m) near the surface. Water (potentially) discharges laterally from each soil layer to the local river reach. Each horizontal grid cell of the model contains only one river reach, and each reach discharges to another reach in the downstream grid cell, following a network that ultimately discharges to the ocean; the sub-grid-scale stream network is ignored. Relations among discharge, storage, velocity, width, and depth in each reach are specified according to Leopold and Maddock (1953).

2.4 Synthesis and Extension of Earlier Developments

For this study, we first combined the lumped N model LM3V-N with the distributed physics of LM3. To complete the N mass balance, we next added a soil denitrification module. Finally, we added stream transport and microbial processes to track the fate of soil N leaching and resolve N dynamics in the aquatic ecosystem. Each of these steps is described below. Figure 1 shows stores and fluxes of N in the resultant model, along with relevant processes. Newly introduced or adjusted parameters from the earlier developments are summarized in Table 1 and variables are listed in Table 2.

2.4.1 Merging lumped N model with distributed physical model

To account for dependence of processes in the lumped soil C and N pools upon the vertically resolved physical states of the soil (temperature and water content), the latter were vertically averaged with an exponentially decaying weight function of depth (e-folding depth of 10 m). Leaching of any mobile constituent was defined as the product of a concentration and the sum

of lateral and vertical discharge from the soil layer between the surface and a depth of 10 m. The concentration of available N was calculated as dividing available N contents by the effective soil depth which was approximated assuming C weight content 3.4% and average soil density 1500 $\mathrm{kg/m^3}$. The available N refers to the N contents reduced by buffering factors which represent processes such as sorption to soil particles. To compensate for many processes that were not accounted for in the model, calibration factors for each N species were introduced to slow down overall N movement from the soil to the stream. These factors include impacts of soil microbes, which are able to take up and incorporate all N forms ($\mathrm{NO_3^- - N}$, $\mathrm{NH_4^+ - N}$, DON) with a much greater capacity than plant uptake (Nordin et al., 2004). The nitrate calibration factor also accounts for storage in groundwater since nitrate (the primary form of N in ground water) can persist for decades at high levels with increasing N applications. This is further explained by Bachman et al. (1998) which reported that 17 to 80 percent of the N delivered to streams of the Chesapeake Bay watershed was through ground water. Furthermore, the lumped single-layer N sub-model bypasses most of the vertically distributed hydrologic system, and the soil N leaching based on the average water drainage is transferred directly from the N layer into the stream. These calibration factors were fit to match inter-annual variations of reported and simulated stream N loads to make up for this modeling approach as well as the unresolved processes that might cause inter-annual stream N loads to be more sensitive to climate variability than those in reality. Considering its importance in groundwater, a relatively larger size of the nitrate N factor is expected. The need to incorporate these calibration factors, which are at the present basin specific, indicates that future improvements to LM3-TAN should focus on resolving these processes (i.e. N cycle in microbes, reservoirs, and vertically distributed soil layers). Dissolved organic, ammonium, and nitrate N leaching from the soil are described as:

$$L_{DON} = \frac{D_s}{\rho_w\, r_{DOM}}\left[N_{DON,av}\right] = \frac{D_s}{\rho_w\, r_{DOM}}\left(\frac{f_{LF}N_{LF} + f_{LS}N_{LS} + f_{SS}N_{SS}}{b_{DOM}\, h_s}\right) \quad (1)$$

$$L_{NH_4^+} = \frac{D_s}{\rho_w\, r_{NH_4^+}}\left[N_{NH_4^+,av}\right] = \frac{D_s}{\rho_w\, r_{NH_4^+}}\left(\frac{N_{NH_4^+}}{b_{NH_4^+}\, h_s}\right) \quad (2)$$

$$L_{NO_s^-} = \frac{D_s}{\rho_w r_{NO_s^-}} \left[N_{NO_s^-,av}\right] = \frac{D_s}{\rho_w r_{NO_s^-}} \left(\frac{N_{NO_s^-}}{b_{NO_s^-} h_s}\right) \quad (3)$$

$$h_s = \frac{C_{LF} + C_{LS} + C_{SS}}{r_c \rho_s} \quad (4)$$

where, L_{DON}, $L_{NH_4^+}$, and $L_{NO_s^-}$ are the dissolved organic, ammonium, and nitrate N leaching from the soil ($\mathrm{kg/m^2\ s}$); D_s is the water drainage from the active soil layer ($\mathrm{kg/m^2\ s}$); ρ_w is the water density (1000 $\mathrm{kg/m^3}$); r_{DOM}, $r_{NH_4^+}$, and $r_{NO_s^-}$ are dissolved organic matter, ammonium, and nitrate N calibration factors; $\left[N_{DON,av}\right]$, $\left[N_{NH_4^+,av}\right]$, and $\left[N_{NO_s^-,av}\right]$ are the concentration of available N in dissolved organic, ammonium, and nitrate N pools ($\mathrm{kg/m^3}$); N_{LF}, N_{LS}, and N_{SS} are the fast litter, slow litter, and slow soil N contents ($\mathrm{kg/m^2}$); f_{LF}, f_{LS}, and f_{SS} are the fractions of soluble organic N in the fast litter, slow litter, and slow soil N pools; $N_{NH_4^+}$ and $N_{NO_s^-}$ are the soil ammonium and nitrate N contents ($\mathrm{kg/m^2}$); b_{DOM}, $b_{NH_4^+}$, and $b_{NO_s^-}$ are dissolved organic matter, ammonium, and nitrate N buffering factors due to sorption to soil particles; h_s is the effective soil depth (m); r_c is the C weight content (3.4%); ρ_s is the average soil density (1500 $\mathrm{kg/m^3}$); C_{LF}, C_{LS}, and C_{SS} are the fast litter, slow litter, and slow soil C contents ($\mathrm{kg/m^2}$).

2.4.2 Denitrification in soil

Denitrification is a process that reduces nitrate or nitrite to gaseous forms (e.g., NO, $\mathrm{N_2O}$, $\mathrm{N_2}$) in anaerobic conditions, where the oxidized N species serve as a terminal electron acceptor in metabolism by soil denitrifying bacteria. The rate of denitrification generally depends on soil nitrate content or concentration, soil water content (a surrogate for oxygen content), and soil

temperature. Because soil nitrate contents are relatively low and limiting under natural conditions, we used a first-order loss function with respect to soil nitrate N content, with adjustments for the influence of soil water content and temperature to simulate soil denitrification rate:

$$D_N = f_S \, f_T \, k_{denitr} \, N_{NO_3^-} \tag{5}$$

where, D_N is the soil denitrification rate ($\mathrm{kg/m^2\ yr}$); f_S is a soil water content reduction function; f_T is a soil temperature reduction function; k_{denitr} is a first-order denitrification coefficient ($1/\mathrm{yr}$); $N_{NO_3^-}$ is the soil nitrate N content ($\mathrm{kg/m^2}$).

$$f_T = Q_{10}^{(T-T_r)/T_p} \tag{6}$$

$$f_S = \begin{cases} S_{min} & S < S_t \\ \left(\frac{S-S_t}{S_{max}-S_t}\right)^w & S_t \leq S \leq S_{max} \\ S_{max} & S_{max} < S \end{cases} \tag{7}$$

where, T is the soil temperature (°C); T_r is a reference temperature (°C); T_p is a parameter; Q_{10} is a factor change in rate with a 10 degree change in temperature; S is the soil water content; S_t is a threshold soil water content; S_{max} is the maximum soil water content; S_{min} is the minimum soil water content; w is an empirical constant.

Heinen (2006) tabulates reported values of the various parameters introduced above. Figure 2 shows the effects of the reduction functions on the soil denitrification rate that were applied in diverse models as well as LM3-TAN. Figure 2a shows how fast soil nitrate N content is reduced to half of the initial amount depending on the different first-order denitrification coefficients. As temperature increases the bacterial activities increase exponentially (Fig. 2b). Soil denitrification occurs and increases non-linearly only if soil water content exceeds a certain threshold point due to enhanced anaerobic bacterial activity (Fig. 2c). The soil water

content reduction function for other microbial processes (e.g., mineralization, nitrification) used in LM3-TAN is also shown in Fig. 2d. Because k_{denitr} is by far the most widely used parameter of these, with reported values ranging over three orders of magnitude, our strategy was to fix the other parameters using reported values, and to calibrate the model by determining k_{denitr} within the bounds reported in the literatures. Because soil denitrification and nitrate-N leaching are competing sinks of nitrate N in the soil, soil denitrification increases as soil nitrate-N leaching or stream nitrate-N load decreases; thus k_{denitr} was fit to match reported and simulated stream nitrate-N loads.

The wide ranges of the functions discussed above are mostly driven by the dependencies of the parameters on specific regions (with different soil properties, vegetation, land use, etc.). Given a number of proposed individual functions, it seems that there is no universal process module to simulate soil denitrification. Because such reduction functions display a diversity of shapes as ecosystems are modeled over a range of climate patterns, vegetation type, and land use practices, soil denitrification on a large scale cannot be modeled without proper adjustments that compensate the site-specific properties. This explains why only a few studies have applied models to watersheds larger than 1000 km^2 despite the diversity of existing dynamic N models and why semi-distributed models often parameterize these individual functions for each of sub-basins in large-scale applications. We hypothesize that LM3-TAN's integrated modeling framework, which is capable of simulating long-term vegetation functional type and land use change as a function of changes in CO_2, climate, and human influences, allows us to use a universal parameter set to simulate soil denitrification for each of the distinct sub-basins. Still, care has to be taken when applying the model to other watersheds that may be very different in terms of soil and climate properties from the Susquehanna watershed. Furthermore, because soil denitrification becomes zero-order in extreme nitrate rich environment, instead of using the first-order loss function for all of the land use types, using a Monod function for agricultural land use may help LM3-TAN's global application where N loadings would vary widely.

2.4.3 Microbial processes in rivers

Despite its importance to water quality, processes that control N removal from water bodies are rarely resolved in watershed scale models, due to both uncertainties in measurement techniques and lack of measurements. To date, none of studies focusing on river denitrification rate is based on measurements of an entire river network, but rather only on the data from low order streams or individual catchments. Here we applied a non-linear regression function based on the LINX (Lotic Intersite Nitrogen experiment; Mulholland et al., 2008) reach-scale measurements that correlates river denitrification rate with nitrate-N concentration and river depth to estimate the reaction rate constant of river denitrification for each reach (Alexander et al., 2009). River denitrification happens mainly in the benthic and/or hyporheic zones. Therefore, a river denitrification rate that is inversely proportional to the river depth accounts for the ratio of water column to benthic area. The measured reaction rate constants vary from 0.034 to 117 ($1/\mathrm{day}$), and we chose the median value 0.53 ($1/\mathrm{day}$) as the minimum reaction rate constant of river denitrification. Equation 12 indicates that the reaction rate constant decreases with increase in nitrate-N concentration and river depth, since both b_1 and b_2 are negative, and it increases with temperature. Reaction rate constants for river mineralization and nitrification were calibrated to match stream N loads.

Figure 1 shows structure of the river component. Each reach directly receives N from point sources (e.g., sewage and waste water discharge) and indirectly receives N from non-point sources (e.g., atmospheric deposition, fertilizer, manure, and legume applications) via soil leaching. The N loads in a reach are routed downstream with the water as following.

$$\frac{dR_{DON}}{dt} = F_{DON}^{in} - F_{DON}^{out} + L_{DON} + P_{DON} - f_T^{'} k_{min}^{'} R_{DON} \quad (8)$$

$$\frac{dR_{NH_4^+}}{dt} = F_{NH_4^+}^{in} - F_{NH_4^+}^{out} + L_{NH_4^+} + P_{NH_4^+} + f_T^{'} k_{min}^{'} R_{DON} - f_T^{'} k_{nitr}^{'} R_{NH_4^+} \quad (9)$$

$$\frac{dR_{NO_3^-}}{dt} = F_{NO_3^-}^{in} - F_{NO_3^-}^{out} + L_{NO_3^-} + P_{NO_3^-} + f_T^{'} k_{nitr}^{'} R_{NH_4^+} - f_T^{'} k_{denitr}^{'} R_{NO_3^-} \quad (10)$$

$$f_T^{'} = T_p^{'(T^{'} - T_r^{'})} \quad (11)$$

$$k_{denitr}^{'} = max\left\{k_{denitr,min}^{'} \ , \ C_{d,s}\left(b_0 {C_{NO_3^-}}^{b_1} H^{b_2} c^t\right)\right\} \quad (12)$$

where, i is DON, NH_4^+, or NO_3^-; R_i is the river N ($\mathrm{kg/m^2}$); F_i^{in} and F_i^{out} is the inflow and outflow of the river N ($\mathrm{kg/m^2\ s}$); L_i is the N leaching from the soil ($\mathrm{kg/m^2\ s}$); P_i is the N point source ($\mathrm{kg/m^2\ s}$); $f_T^{'}$ is the stream temperature reduction function; $T^{'}$ is the water temperature (°C); $T_r^{'}$ is the reference water temperature (°C); $T_p^{'}$ is a parameter; $k_{min}^{'}$, $k_{nitr}^{'}$, and $k_{denitr}^{'}$ are the reaction rate constants for river mineralization, nitrification, and denitrification ($1/\mathrm{s}$); $k_{denitr,min}^{'}$ is the minimum reaction rate constant of river denitrification ($1/\mathrm{s}$); $C_{NO_3^-}$ is the nitrate N concentration ($\mu\mathrm{mol\ N/l}$); H is the river depth (m); b_0, b_1, and b_2 are the constants; c^t is the log re-transform bias correction factor; $C_{d,s}$ is a unit-conversion constant.

3 Study site

The Susquehanna River basin, where nearly four million people live, is the largest of the watersheds in the northeastern U.S. and drains an area of 71,220 square kilometers, contributing two-thirds of the annual N load to the Chesapeake Bay (Fig. 3). The basin includes 2,293 lakes, reservoirs, and ponds (322 $\mathrm{km^2}$) as well as 50,190 kilometers of rivers and streams. The main stem of the Susquehanna River originates at Otsego Lake, N.Y., and flows about 750 kilometers through New York, Pennsylvania, and Maryland to the Chesapeake Bay at Havre de Grace, Md. The Susquehanna Large River Assessment Project reported that only 6.9 percent of water quality values exceeded their standards, but the majority of these exceedances were for nutrients (e.g. TN, TP) (Hoffman, 2009), explaining why the Chesapeake Bay suffers from nutrient enrichment problems and hypoxia.

The reported 2000 land use is about 63 percent forest or wooded, 19 percent crop land, 7 percent pasture, 9 percent urban, and 2 percent water. The Upper Susquehanna River flows through mostly forested and agricultural land with some small communities and one larger population center, then confluences with the Chemung River at Sayre, Pa. The West Branch Susquehanna Sub-basin is mostly woods and grasslands. The Middle Susquehanna River, from the confluences with the Chemung River at Sayre, Pa. to the confluences with the West Branch Susquehanna River at Sunbury, Pa., flows along very diverse land use. The Lower Susquehanna Sub-basin contains extensive agriculture and several large population centers. The other major urban areas are found within the Juniata Sub-basin (Hoffman, 2008).

The geology of the watershed is mainly clastic sedimentary rock of sandstone and shale. Elevations vary from 30 meters at the Chesapeake Bay in Maryland to 955 meters in central New York State (McGonigal, 2011). The Great Lakes and Midwest climate exert influence over the Upper Susquehanna, Chemung, and West Branch Susquehanna Sub-basin, whereas the Atlantic coastal climate affect on the other portions of the watershed. The basin has experienced severe droughts about once every decade, and the worst droughts occurred in 1930, 1939 and 1964. The basin is also one of the most flood-prone watersheds in the nation with frequent and localized flash floods every year. The worst recorded flooding in the basin happened in 1972 as a result of tropical storm Agnes.

4 Stream Sampling Description

Stream discharge data are provided by the network of stream gauges operated by the U.S. Geological Survey (USGS), which collects and summarizes time series data to derive annual, monthly, and daily stream discharge and statistics (Fig. 3). mode were monitored by the USGS and Susquehanna River Basin Commission (SRBC). One USGS and six SRBC long-term nutrient monitoring sites monitored since 1985 and 9 newly introduced SRBC sites monitored since either 2004 or 2005 to present (Table 3; Fig. 3; McGonigal, 2011; USGS, 2014) were chosen for model evaluation. The 16 sites vary in sub-basin area and land use. Among the USGS and SRBC sites, the Conowingo and Marietta sites on the main channel of the Susquehanna River have the largest sub-basin areas respectively (70,189 and 67,314 km^2). The sub-basin of the Conestoga site contains extensive agriculture (48%) and the most

populated urban land use with several large population centers (24%) within a very small area (1,217 km^2). The West Branch River flows mostly along woods and grasslands to the Lewisburg site. The long-term sites have collected two samples per month. Additional samplings are made during seasonal storm conditions. The collected water samples are analyzed for various N species: dissolved N (DN), dissolved nitrite and nitrate (DNO_{23}), dissolved ammonia (DNH_3), dissolved organic N (DON), and dissolved ammonia and organic N (DKN) in milligrams per liter. In addition, annual, seasonal, and monthly loads are computed by the Minimum Variance Unbiased Estimator (ESTIMATOR; SRBC, 2006; USGS, 2014). River temperatures were reported when the samplings were collected for the chemical analysis of stream waters.

5 Anthropogenic N sources

Anthropogenic N data over the two decades (1985-2005) were provided by the Chesapeake Community Modeling Program (CCMP). Atmospheric deposition data were provided by the county-based land segments. Fertilizer, manure, and legume applications as well as combined sewer overflows (CSOs) were provided by the land-river segments of the GIS-based Phase 5.3 Community Watershed Model (USEPA, 2010a). The atmospheric deposition data were calculated by the Chesapeake Bay Program (CBP) Airshed Model, which is a combination of a regression model of wet deposition (Grimm and Lynch, 2005) and the Community Multiscale Air Quality Model (CMAQ) that estimates dry deposition (Dennis et al., 2007; Hameedi et al., 2007). The fertilizer, manure, and legume data were estimated for the years of 1985, 1987, 1992, 1997, 2002, and 2005 by the Scenario Builder Version 2.2, a process based model that is designed to use agricultural censuses as a main input data (USEPA, 2010b). The agricultural censuses were produced by the United States Department of Agriculture National Agricultural Statistics Service (NASS) and include data of animal populations, farms, agricultural land areas, and crop yields. The point sources were estimated by 42 CSO communities within the Susquehanna basin, using either various versions of EPA's Storm Water Management Model (SWMM) or spatial data collected as a result of a direct survey of the communities (USEPA, 2010a). The detailed data description can be found in the Phase 5.3 Community Watershed Model documentation (USEPA, 2010a).

Over the two decades, the total N sources decreased by about 20 percent. The atmospheric deposition was predominantly nitrate-N accounting for about 69 percent; ammonium-N 27 percent; organic-N 4 percent. The sum of the fertilizer, manure, and legume applications consisted of 49 percent of ammonium-N, followed by 37 percent organic-N, and 14 percent nitrate-N. Especially, the ammonium-N and organic-N loads had considerable variability across the spatial domain because they were strongly influenced by local emissions from the extensive agricultural areas.

Figure 4 shows spatial distribution maps of the applied anthropogenic N sources, which were calculated as a spatial resolution of 0.125° by 0.125° and a temporal resolution of one year. For each grid cell, which consists of up to 15 land-use tiles, atmospheric depositions (nitrate-N, ammonium-N, and organic-N) were applied to all of the land tiles, and fertilizer, manure, and legume applications (nitrate-N, ammonium-N, and organic-N) were applied only to the crop land tiles. Combined sewer overflows (nitrate-N, ammonium-N, and organic-N) were directly applied to the river reaches. The 20-year (1986-2005) average non-point and point N sources for the six sub-basins are summarized in the Table 4. The thick solid arrows in Fig. 1 depict fluxes of each of N species for the anthropogenic N sources to the corresponding terrestrial and river pools respectively.

6 Model forcing and simulations

The model was implemented with a spatial resolution of 0.125° by 0.125° with time increments of 30 minutes. The model was forced using reported hydrological data cycled over a horizon of 61 years (1948-2008) to perform long-term simulations. The data include precipitation, specific humidity, air temperature, surface pressure, wind speed, and short and long wave downward radiation with a spatial resolution of 1° by 1°on timescales of 3 hours (Sheffield et al., 2006). Land-use change was simulated from 1704 to 2005 using a scenario of land use transitions (Hurtt et al., 2006). Preindustrial CO_2 concentration assumed as 286 ppm

was applied from 1704 to 1799, and changes in CO_2 concentrations were applied from 1800 to 2005 using reported data from NOAA's Earth System Research Laboratory. For 250 years (1704-1953), the estimated preindustrial N deposition (Dentener and Crutzen, 1944; Green et al., 2004; Gerber et al., 2010) was applied as a uniform annual rate. We then applied the reported 1985's anthropogenic N data from 1954 to 1984, and reported annual anthropogenic N data from 1985 to 2005.

7 Result and Discussion

7.1 Evaluation of stream waters and N loads

We simulated with LM3-TAN stream dissolved organic-N, ammonium-N, and nitrate-N loads throughout the river network. The model was calibrated by comparing the modeled stream N loads with the corresponding reported N loads at the last downstream SRBC station Marietta, in which contributions of the entire watershed to the stream flows and N loads can be assessed. Thus, temporal evaluation of the stream discharges and N loads for the period 1987-2005 was focused on at the Marietta station. River data from the 16 monitoring stations (1986-2005) were also used to evaluate spatial stream discharges and N loads.

Using global hydrological data and a universal parameter set for the entire watershed, the model produced reasonable temporal patterns of annual stream discharge. The simulated stream discharges were in a good agreement with the reported values in dry years and periods (July to September), but under-estimated stream discharges in wet years and periods (March to May). Overall, although the 19-year average simulated discharge was about 28% lower than the corresponding reported value, their linear and rank correlations were significantly high (Table 5), implying that the bias was systemic and accounted for in the calibration of the N species.

Due to their complex physical and biogeochemical interactions with soil particles and soil organic matter, simulating reactive transport of ammonium and dissolved organic N is far more challenging than simulating nitrate N transport. For example, the correlation at Marietta

between stream discharge and nitrate N load ($R^2 = 0.98$) was significantly higher than that for dissolved organic N (R^2 = 0.48) or for ammonium N ($R^2 = 0.85$) loads, implying that in addition to the hydrological processes governing soil N transport to rivers, terrestrial physical and microbial processes (e.g., sorption to soil particles, organic matter decomposition and stabilization) have to be accounted for when estimating stream ammonium and dissolved organic N loads. This, plus the fact that the highest component in the overall stream N load is nitrate N, explains why existing watershed models have focused on stream nitrate N loads, and neglected ammonium and dissolved organic N loads. Within the LM3-TAN's integrated modeling framework, we estimated all of the N species for the entire drainage network.

At Marietta, 19 year average simulated stream dissolved-N (-0.5%), nitrate-N (-0.2%), ammonium-N (+4.7%), and dissolved organic-N (-2.6%) loads were close to the corresponding reported values. Both of the simulated and monitored dissolved-N loads consisted of predominantly nitrate N (79%), followed by dissolved organic-N (18%), and ammonium-N (3%). The model also produced reasonable temporal patterns of annual dissolved-N (r = 0.7), nitrate-N (r = 0.6), ammonium-N (r = 0.7), and dissolved organic-N (r = 0.6) loads (Fig. 5; Table 5). At Conowingo, 20 year average simulated nitrate-N load agreed well with the corresponding reported value (-3.7%), but the model, which doesn't have lakes or reservoirs, fails to capture inter-annual variations of the loads (r = 0.2), which are affected by the reservoir system between the Marietta and Conowingo monitoring sites (Fig. 5).

Simulated and reported dissolved -N loads were graphed in different units: millions of kg/yr and kg/km^2 yr (normalized by its sub-basin area summarized in Table 3). Among the 6 long-term monitoring sites, the highest and lowest amount of river N loads were reported and simulated at the Marietta and Conestoga sites respectively (Fig. 6a). This finding is consistent with the general view that the amount of stream N loads is proportional to size of the basin area. A very high N flux was reported at the Conestoga site (Fig. 6b), which can be explained by its sub-basin's extensive agriculture and urban land use. Because the West Branch Susquehanna is dominated mostly by woods and grasslands, the Lewisburg site had the lowest

N flux. The model also captured the stream N loads at the 15 monitoring sites well (Fig. 6c and 6d). These results attest to the model ability to correctly simulate the stream N loads for the entire basin based on the climate as well as land use and the corresponding N sources and transformations in the sub-basins.

7.2 Spatial distribution of stream N load and soil denitrification rate

Observation of the spatial distribution of the river N load (Fig. 7) and soil denitrification rate (Fig. 8d) helps to identify the extent of the terrestrial and aquatic N pollution across the basin. A large amount of N is exported via the main stem of the Susquehanna River as well as its three major tributaries, where many small-order streams converge. The N loads in the streams increase gradually from the headwaters to the watershed outlet, implying that the N loads to the rivers exceed N removal mechanisms within the rivers. Although stream N loads are in general higher in the larger rivers, at the Lower Susquehanna sub-basin, high N loads are present even in small-order streams due to the extensive agricultural land use.

Figure 8 presents 20 year average (1986-2005) simulated soil water content, temperature, nitrate-N content, and denitrification rate, and these for each of 6 sub-basins as well as the corresponding sub-basin area, non-point and point N sources are summarized in Table 4. An analysis for the 6 sub-basins shows that the combined effects of land use and climate on the soil denitrification rate, which were the highest in the Lower Susquehanna Sub-basin (extensive agriculture; Atlantic coastal climate) and the lowest in the West Branch Susquehanna Sub-basin (mostly forest; Great Lakes and Midwest climate). These results show that the most significant soil denitrification is associated with extensive agricultural land use (non-point sources). The calculated R^2 statistic between the monthly soil denitrification rate and soil water content ($R^2 = 0.51$) was significantly higher than that for soil temperature or soil nitrate N content, implying that the soil water content played the greatest role in the soil denitrification process among the three factors. This is because the soil denitrification occurred and increased non-linearly only when the soil water content exceeded the threshold point ($S_t = 0.577$). The significant effect of the soil water content on the soil denitrification is

further illustrated in the upper east side of the Upper Susquehanna Sub-basin, where extremely low soil water content (Fig. 8a) impeded the overall soil denitrification process (Fig. 8d).

7.3 N budget

As a further means of evaluating the model output, we compared the simulated N budget for the period 1988-1992 to the budget constructed by Boyer et al. (2002), Seitzinger et al., (2002), and Van Breemen et al., (2002) for the same period (Fig. 9). Overall, reasonable agreements were found between these two budgets. Total N inputs to the whole basin were reported as 4,774 ($kg/km^2\ yr$; atmospheric deposition + fertilizer + forest and agricultural N fixation + net N import in feed and food), while we applied 4,443 of N ($kg/km^2\ yr$; atmospheric deposition + fertilizer + manure + legume + sewage) using the data sources provided by CCMP (USEPA 2010a). The simulated soil denitrification (-4%), harvest rates (+7%), river export (-1%), and river denitrification (-5%) agreed well with the corresponding reported values. To investigate the importance of N removal within rivers, we ran an experiment in which the reaction rate constant for river denitrification was set to zero. We then compared N loads within the rivers with and without river denitrification. Figure 10 shows a spatial map of the difference in N loads between these simulations, which represents the river N removal. A large amount of N was removed along the main stem of the Susquehanna River as well as its three major tributaries, implying that the N removal increases gradually as distance from the headwaters increases. About 28 percent of the N that enters to the rivers was removed by river denitrification.

For the entire basin, we divided the simulated land use into either agricultural land (cropland and pasture) or secondary forest (land formerly disturbed by human activities). We then graphed simplified N budgets for each land use (Fig. 9c). The reported agricultural land use was 29 percent (Fig. 9a), whereas the model simulated 24 percent of cropland and pasture (Fig. 9b). In the secondary forest land, most of the applied N (43%) was stored in the terrestrial system (vegetation and soil pools), whereas the highest proportion of the applied N was removed by soil denitrification (44%) in the agricultural land. These results imply that

applications of artificial N to agricultural lands can result in considerable soil denitrification rates, and thus significant increase of N_2O production. This is evident when comparing maps of the applied fertilizer, manure, and legume N applications (Fig. 4c and 4d) and the simulated soil denitrification (Figure 8d) that corresponds well, especially in the Lower Susquehanna Sub-basin with extensive agricultural land use. Even if there are some discrepancies between these two budgets, we can conclude that the reactive transport of N from the terrestrial to aquatic ecosystems was appropriately simulated by the model, providing suitable descriptive information for the entire drainage network.

8 Conclusions

Results of our study show that LM3-TAN captures well the key mechanisms that control N dynamics in the climate-plant-soil-river system. Specifically, we demonstrate:

- On a sub-basin scale with different climate and land-use regimes, the LM3-TAN properly simulates terrestrial N cycling, including effects of long-term vegetation dynamics, land-use changes, and hydrological cycles. The interaction among those three processes allow LM3-TAN to capture soil C-N organic matter and mineral N transformations as well as soil emissions of nitrate-N and leaching of dissolved organic, ammonium, and nitrate N.
- The ability to capture N soil budget and losses then enables LM3-TAN to consistently characterize trends and variability in riverine N inputs and exports of ammonium, dissolved organic, and nitrate N with explicit representation of their transformations and transport in rivers.
- In the re-growing secondary forests, a large fraction of the N from atmospheric deposition has been stored in the vegetation and soil, but in the agricultural lands most N inputs were removed by soil denitrification indicating that anthropogenic N inputs could drive substantial increase of N_2O emission, an intermediate of the denitrification process.
- LM3-TAN captures effects of long-term trends and variability of hydrological cycles (e.g., precipitation, soil water content, stream discharge) on N cycling in vegetation-soil-river system, and thus resolves inter-annual variations of stream N loadings caused by climate variability.

- The model results suggest that the soil denitrification is most sensitive to soil water variations.
- Among the 6 sub-basins, the soil denitrification rate was the highest in the Lower Susquehanna Sub-basin with the most intensive land-use non-point N sources as well as with the warmest and wettest soils, attributed to the Atlantic coastal climate.
- Even though the N denitrification and riverine biogeochemistry N modules were calibrated only at the last downstream station Marietta, application of the universal parameters at the entire watershed produced simulations which compared well at other observational stations. The applicability of the universal parameters in other watersheds is a subject of the future research.
- This study shows that linking terrestrial N and C cycling, long-term land-use and vegetation dynamics, and hydro-climate variations to N loads and concentrations in streams, provides an effective and consistent framework for analysis of the surface water N processes and water quality for large watersheds and basins.

Acknowledgements

We thank K. A. Dunne from USGS for providing the 1/8 degree river network dataset. We thank J. Blomquist from USGS, K. McGonigal from the Susquehanna River Basin Commission, G. A. Yactayo from the Chesapeake Bay Program for providing river N-load or anthropogenic N input data and assisting with their interpretation. We thank reviewers for their insightful and helpful comments.

Support for M. Lee was provided by a Fulbright Scholarship, by the Princeton Environmental Institute at Princeton University through the Mary and Randall Hack '69 Research Fund, and by the Korean National Institute of Environmental Research. E. Shevliakova and S. Malyshev acknowledge support in parts from the NOAA (U.S. Department of Commerce) grant NA08OAR4320752 and the USDA grant 2011-67003-30373. The statements, findings, and conclusions are those of the authors and do not necessarily reflect the views of the NOAA, the U.S. Department of Commerce, and the U.S. Department of Agriculture.

References

Albritton, D. L., Derwent, R. G., Isaksen, I. S. A., Lal, M., and Wuebles, D. J.: Trace gas radiative forcing indices, in: Climate Change 1994: Radiative Forcing of Climate Change and an Evaluation of the IPCC IS92 Emission Scenarios, Houghton, J. T., Cambridge University Press, Cambridge, U. K., 205-231, 1995.

Alexander, R. B., Böhlke, J. K., Boyer, E. W., David, M. B., Harvey, J. W., Mulholland, P. J., Seitzinger, S. P., Tobias, C. R., Tonitto, C., Wollheim, W. M.: Dynamic modeling of nitrogen losses in river networks unravels the coupled effects of hydrological and biogeochemical processes, Biogeochem., 93, 91–116, 2009.

Bachman, L. J., Lindsey, B. D., Brakebill, J. W., and Powars, D. S.: Ground-water discharge and base-flow nitrate loads of non tidal streams, and their relation to a hydrogeomorphic classification of the Chesapeake Bay watershed, U.S. Geological Survey Water-Resources Investigations Rep. 98–4059, 71 pp., 1998.

Band, L. E., Tague, C. L., Groffman, P., and Belt, K.: Forest ecosystem processes at the watershed Scale: hydrological and ecological controls of nitrogen export, Hydrol. Processes, 15, 2013-2028, 2001.

Beckers, J., Smerdon, B., and Wilson, M.: Review of hydrologic models for forest management and Climate change applications in British Columbia and Alberta, FORREX SERIES 25, FORREX Forum for Research and Extension in Natural Resources Society, Kamloops, B. C., 2009.

Bolker, B. M., Pacala, S. W., and Parton, W. J.: Linear analysis of soil decomposition: Insights from the CENTURY model, Ecol. Appl., 8, 425-439, 1998.

Boyer, E. W., Goodale, C. L., Jaworski, N. A., and Howarth, R. W.: Anthropogenic nitrogen sources and relationship to riverine nitrogen export in the northeastern U. S. A., Biogeochem., 57–58, 137–169, 2002.

Bril, J., van Faassen, H. G., Klein Gunnewiek, H.: Modeling N2O Emission from Grazed Grassland, Report 24, Institute for Agrobiology and Soil Fertility, Wageningen, The Netherlands, 1994.

Chesapeake Community Modeling Program: http://ches.communitymodeling.org/index.php, last access: 17 January 2010.

Del Grosso, S. J., Ojima, D. S., Parton, W. J., Stehfest, E., Heistemann, M., DeAngelo, B., and Rose, S.: Global scale DAYCENT model analysis of greenhouse gas emissions and mitigation strategies for cropped soils, Global and Planet. Change, 67, 44-50, 2009.

Dennis, R., Haeuber, R., Blett, T., Cosby, J., Driscoll, C., Sickles, J., and Johnson, J.: Sulfur and nitrogen deposition on ecosystems in the United States, EM: The Magazine for Environmental Managers, December 2007, 12-17, 2007.

Dentener, F. J. and Crutzen, P. J.: A three-dimensional model of the global ammonia cycle, J. Atmos. Chem, 19, 331–369, 1994.

Dunne, J. P., John, J. G., Adcroft, A. J., Griffies, S. M., Hallberg, R. W., Shevliakova, E., Stouffer, R. J., Cooke, W., Dunne, K. A., Harrison, M. J., Krasting, J. P., Malyshev, S. L., Milly, P. C. D., Phillipps, P. J., Sentman, L. T., Samuels, B. L., Spelman, M. J., Winton, M., Wittenberg, A. T., and Zadeh, N.: GFDL's ESM2 global coupled climate-carbon Earth System Models. Part I: Physical formulation and baseline simulation characteristics, J. Climate, 25, 6646–6665, 2012.

Galloway, J. N., Dentener, F. J., Capone, D. G., Boyer, E. W., Howarth, R.W., Seitzinger, S. P., Asner, G. P., Cleveland, C. C., Green, P. A., Holland, E. A., Karl, D. M., Michaels, A. F., Porter, J. H., Townsend, A. R., and Vorosmarty, C. J.: Nitrogen cycle: past, present, and future, Biogeochemistry, 70, 153-226, 2004.

Galloway, J. N., Townsend, A. R., Erisman, J. W., Bekunda, M., Cai, Z., Freney, J. R., Martinelli, L. A., Seitzinger, S. P., and Sutton, M. A.: Transformation of the Nitrogen Cycle: Recent Trends, Questions, and Potential Solutions, Science, 320, 889-892, 2008.

Gerber, S., Hedin, L. O., Oppenheimer, M., Pacala, S. W., and Shevliakova, E.: Nitrogen cycling and feedbacks in a global dynamic land model, Global Biogeochem. Cycles, 24, GB1001, doi:10.1029/2008GB003336, 2010.

Green, P. A., Vorosmarty, C. J., Meybeck, M. J., Galloway, N., Peterson, B. J., and Boyer, E.W.: Pre-industrial and contemporary fluxes of nitrogen through rivers: A global assessment based on typology, Biogeochem., 68, 71– 105, 2004.

Grimm, J. W. and Lynch, J. A.: Improved daily precipitation nitrate and ammonium concentration models for the Chesapeake Bay Watershed, Environ. Pollut., 135, 445-455, 2005.

Hameedi, J., Paerl, H., Kennish, M., Whitall, D.: Nitrogen deposition in U. S. coastal bays and estuaries, EM: The Magazine for Environmental Managers, December 2007, 19-25, 2007.

Heinen, M.: Simplified denitrification models: Overview and properties, Geoderma, 133, 144-463, 2006.

Henriksen, A. and Brakke, D. F.: Increasing contributions of nitrogen to the acidity of surface waters in Norway, Water Air Soil Pollut., 42, 183-202, 1988.

Hoffman, J. L. R.: The 2008 Susquehanna River basin water quality assessment report, Susquehanna River Basin Commission, Harrisburg, Pennsylvania, 2008.

Hoffman, J. L. R.: Susquehanna large river assessment project, Publication 265, Susquehanna River Basin Commission, Harrisburg, Pennsylvania, 2009.

Howarth, R.W.: Nutrient over-enrichment of coastal waters in the United States: Steps toward a solution, Pew Oceans Commission, Washington, DC., 2002.

Howarth, R. W., Swaney, D. P., Boyer, E. W., Marino, R., Jaworski, N., and Goodale, C.: The influence of climate on average nitrogen export from large watersheds in the Northeastern United States, Biogeochem., 79, 163-186, 2006.

Hurtt, G. C., Frolking, S., Fearon, M. G., Moore, B., Shevliakova, E., Malyshev, S., Pacala, S. W., and Houghton, R. A.: The underpinnings of land-use history: three centuries of global gridded land-use transitions, wood-harvest activity, and resulting secondary lands, Global Change Biol., 12, 1208–1229, 2006.

Johnsson, H., Bergstrom, L., Jansson, P., Paustian, K.: Simulated nitrogen dynamics and losses in a layered agricultural soil, Agric. Ecosyst. Environ., 18, 333– 356, 1987.

Kelly, C. A., Rudd, J. W. M., and Schindler, D.W.: Acidification by nitric acid: future Considerations, Water Air Soil Pollut., 50, 49-61, 1990.

Kroes, J. G. and Roelsma, J.: User's guide for the ANIMO version 3.5 nutrient leaching Model, Technical Document 46, DLO-Staring Centrum, Wageningen, The Netherlands, 1998.

Leadley, P. W., Reynolds, J. F., and Chapin, F. S.: A model of nitrogen uptake by Eriophorum vaginatum roots in the field: Ecological implications, Ecological Monographs, 67, 1-22, 1997.

Neff, J. C. and Asner, G. P.: Dissolved organic carbon in terrestrial ecosystems: Synthesis and a model, Ecosystems, 4, 29-48, 2001.

Leopold, L. B. and Maddock T.: The hydraulic geometry of stream channels and some physiographic implications, U. S., Geol. Surv. Prof. Paper, 252, 57, 1953.

McGonigal, K. H.: 2010 nutrients and suspended sediment in the Susquehanna River basin, Susquehanna River Basin Commission, Harrisburg, Pennsylvania, 2011.

Milly, P. C. D., Malyshev, S. L., Shevliakova, E., Dunne, K. A., Findell, K. L., Gleeson, T., Liang, Z., Phillips, P., Stouffer, R. J., and Swenson, S.: An enhanced model of land water and energy for global hydrologic and earth-system studies, J. Hydrometeorol, doi: http://dx.doi.org/10.1175/JHM-D-13-0162.1, 2014.

Mulholland, P. J., Helton, A. M., Poole, G. C., Hall, R. O., Hamilton, S. K., Peterson, B. J., Tank, J. L., Ashkenas, L. R., Cooper, L. W., Dahm, C. N., Dodds, W. K., Findlay, S. E. G, Gregory, S. V., Grimm, N. B., Johnson, S. L., McDowell, W. H., Meyer, J. L., Valett, H. M., Webster, J. R., Arango, C. P., Beaulieu, J. J., Bernot, M. J., Burgin, A. J., Crenshaw, C. L., Johnson, L. T., Niederlehner, B. R., O'Brien, J. M., Potter, J. D., Sheibley, R. W., Sobota, D. J., and Thomas, S. M.: Stream denitrification across biomes and its response to anthropogenic nitrate loading, Nature, 452, 202–205, 2008.

Murdoch, P. S. and Stoddard, J. L.: The role of nitrate in the acidification of streams in the Catskill Mountains of New York, Water Resour. Res., 28, 2707-2720, 1992.

NOAA (National Oceanic and Atmospheric Administration)'s Earth System Research Laboratory: available at: www.esrl.noaa.gov/gmd/ccgg/trends (last access: 21 Feburary 2014), 2011.

Nordin, A., Schmidt, I. K., and Shaver, G. R.: Nitrogen uptake by arctic soil microbes and plants in relation to soil nitrogen supply, Ecology, 85, 955–962, 2004.

Parton, W. J., Scurlock, J. M. O., Ojima, D. S., Gilmanov, T. G., Scholens, R. J., Schimesl, D. S., Kirchner, T., Menaut, J-C., Seastedt, T., Moya, E. G., Kamnalrut, A., and Kinyamario, J. I.: Observations and modeling of biomass and soil organic matter dynamics for the grassland biome worldwide, Global Biogeochem. Cycles, 7, 785– 809, 1993.

Scavia D., Field J. C., Boesch, D. F., Buddemeier, R. W., Burkett, V., Canyan, D. R., Fogarty, M., Harwell, M. A., Howarth, R.W., Mason, C., Reed, D. J., Royer, T. C., Sallenger, A. H.,

and Titus, J. G.: Climate change impacts on U. S. coastal and marine ecosystems, Estuaries, 25, 149–164, 2002.

Schilling, K. E. and Wolter, C. F.: Modeling nitrate-nitrogen load reduction strategies for the Des Moines River, Iowa using SWAT, J. Environ. Manage, 44, 671-82, 2009.

Seitzinger, S. P., Styles, R. V., Boyer, E., Alexander, R. B., Billen, G., Howarth, R., Mayer, B., Van Breemen, N.: Nitrogen retention in rivers: model development and application to watersheds in the eastern US, Biogeochem., 57/58, 199–237, 2002.

Sharpley, A. N. and Williams J. R.: EPIC erosion/productivity impact calculator: 1. Model Documentation, Technical Bulletin No. 1768, U. S. Department of Agriculture, Temple, Texas, U. S. A, 1990.

Sheffield, J., Goteti, G., and Wood, E. F.: Development of a 50-yr high-resolution global dataset of meteorological forcings for land surface modeling, J. Climate, 19, 3088-3111, 2006.

Shevliakova, E., Pacala, S. W., Malyshev, S., Hurtt, G. C., Milly, P. C. D., Caspersen, J. P., Sentman, L. T., Fisk, J. P., Wirth, C., and Crevoisier, C.: Carbon cycling under 300 years of land use changes: Importance of the secondary vegetation sink, Global Biogeochem. Cycles, 23, GB2022, doi:10.1029/2007GB003176, 2009.

Smith, V. H.: Eutrophication of freshwater and marine ecosystems: a global problem, Environ. Sci. Pollut. Res., 10, 126–139, 2003.

Smith, V. H., Joye, S. B., and Howarth, R.W.: Eutrophication of freshwater and marine ecosystems, Limnol. Oceanogr. 51, 351–355, 2006.

Sogn, T. A. and Abrahamsen, G.: Simulating effects of S and N deposition on soil water chemistry by the nutrient cycling model NuCM, Ecol. Modell., 99, 101– 111, 1997.

SRBC (Susquehanna River Basin Commission): available at: http://www.srbc.net/ (last access: 17 January 2014), 2006.

Tague, C. L. and Band, L. E.: RHESSys: regional hydro-ecologic simulation system-An object-oriented approach to spatially distributed modeling of carbon, water, and nutrient cycling, Earth Interact., 8, 1–42, 2004.

Thomas, R. Q., Bonan, G. B., and Goodale, C. L.: Insights into mechanisms governing forest carbon response to nitrogen deposition: a model–data comparison using observed responses to nitrogen addition, Biogeosciences, 10, 3869–3887, 2013.

Thornton, P. E., Lamarque, J., Rosenbloom, N. A., and Mahowald, N. M.: Influence of carbon-nitrogen cycle coupling on land model response to CO2 fertilization and climate variability, Global Biogeochem. Cycles, 21, GB4018, doi:10.1029/2006GB002868, 2007.

USEPA (U. S. Environmental Protection Agency): Chesapeake Bay Phase 5.3 Community Watershed Model, EPA 903S10002 - CBP/TRS-303-10, U. S. Environmental Protection Agency, Chesapeake Bay Program Office, Annapolis, MD, 2010a.

USEPA (U. S. Environmental Protection Agency): Estimates of county-level nitrogen and phosphorus data for use in modeling pollutant reduction: Documentation for Scenario Builder Version 2.2. CBP/TRS 903R100004 Bin # 304, U. S. Environmental Protection Agency Chesapeake Bay Program Office, Annapolis MD, 2010b.

USGS (US Geological Survey): available at: http://www.usgs.gov/ (last access: 17 January 2014), 2009.

USGS (US Geological Survey): available at: http://cbrim.er.usgs.gov/loads_query.html (last access: 28 July 2014), 2014.

Van Breemen, N., Boyer, E. W., Goodale, C. L., Jaworski, N. A., Paustian, K., Seitzinger, S., Lajtha, L. K., Mayer, B., Van Dam, D., Howarth, R. W., Nadelhoffer, K. J., Eve, M., Billen, G.: Where did all the nitrogen go? Fate of nitrogen inputs to large watersheds in the northeastern U. S. A., Biogeochem., 57/58, 267–293, 2002.

Wade, A. J., Durand, P., Beaujouan, V., Wessel, W.W., Raat, K. J., Whitehead, P. G., Butterfield, D., Rankinen, K., and Lepisto, A.: Nitrogen model for European catchments: INCA, new model structure and equations, Hydrol. Earth Syst. Sci., 6, 559-582, 2002.

Williams, J. R.: The EPIC model in: Computer Models of Watershed Hydrology, Singh, V. P., Water Resources Publications, Highlands Ranch, Colorado, USA, 1995.

1 Table 1. Newly introduced or adjusted parameters from the earlier developments.

Parameter	Description	Value	Unit	Reference or Rationale
Parameters in the Land Component Equations				
b_{DOM}, $b_{NH_4^+}$, $b_{NO_3^-}$	buffering factors for DOM, ammonium-N, nitrate-N	3, 5, 1	unitless	Leadly et al., 1997; Neff and Asner, 2001
f_{DOM}	fraction of litter soil decomposition that becomes potential DOM (Gerber et al., 2010)	0.034	unitless	calibrated to match stream DON loads; Gerber et al., 2010
k_{denitr}	first-order denitrification coefficient	6.5	$1/yr$	Heinen, 2006
r_{DOM}, $r_{NH_4^+}$, $r_{NO_3^-}$	calibration factors for DOM, ammonium-N, nitrate-N	10, 20, 100	unitless	calibrated to match inter-annual variations of stream N loads
q_{max}	transfer fractions form slow litter to slow soil (Gerber et al., 2010)	0.6	unitless	Parton et al., 1993; Bolker et al., 1998; Gerber et al., 2010
q_{SP}	transfer fractions form slow litter to passive soil (Gerber et al., 2010)	0.004	unitless	Parton et al., 1993; Bolker et al., 1998; Gerber et al., 2010
S_{min}	minimum soil water content	0	unitless	Bril et al., 1994; Heinen, 2006
S_{max}	maximum soil water content	1	unitless	Bril et al., 1994; Heinen, 2006
S_t	threshold soil water content	0.577	unitless	Bril et al., 1994; Heinen, 2006
w	empirical constant	2	unitless	Bril et al., 1994; Heinen, 2006
T_p	parameter	10	unitless	Sogn and Abrahamsen, 1997; Johnsson et al., 1987; Heinen, 2006
T_r	reference temperature	15	°C	Sogn and Abrahamsen, 1997; Johnsson et al., 1987; Heinen, 2006

Q_{10}	factor change in rate with a 10 degree change in temperature	2	unitless	Sogn and Abrahamsen, 1997; Johnsson et al., 1987; Heinen, 2006
Parameters in the River Component Equations				
b_0, b_1, b_2	constants	0.559, -0.478, -0.612	unitless	Alexander et al., 2009
c^t	log re-transform bias correction factor	1.90	unitless	Alexander et al., 2009
$k'_{denitr,min}$	minimum reaction rate constant of river denitrification	0.53/86400	$1/s$	Alexander et al., 2009
$C_{d,s}$	unit-conversion constant	1/86400	day/s	conversion from $1/day$ to $1/s$
k'_{min}, k'_{nitr}	reaction rate constants for river mineralization, nitrification	0.11/86400, 0.51/86400	$1/s$	calibrated to match stream N loads
T'_p	parameter	1.047	unitless	Wade et al., 2002
T'_r	reference water temperature	20	°C	Wade et al., 2002

Table 2. Definition of prognostic (PV) and diagnostic (DV) variables and inputs/forcings (IF) used in the equations.

Vegetation and Soil Equations			
C_{LF}, C_{LS}, C_{SS}	PV	fast litter, slow litter, slow soil C contents	kg/m^2
D_N	DV	soil denitrification rate	kg/m^2 yr
D_s	DV	water drainage from active soil layer	kg/m^2 s
f_{LF}, f_{LS}, f_{SS}	PV	fractions of soluble organic N in the fast litter, slow litter, slow soil N pools (Gerber et al., 2010)	unitless
f_S	PV	soil water content reduction function	unitless
f_T	PV	soil temperature reduction function	unitless
h_s	PV	effective soil depth	m
$L_{DON}, L_{NH_4^+}, L_{NO_3^-}$	PV	soil leaching for DON, ammonium-N, nitrate-N	kg/m^2 s
$[N_{DON,av}], [N_{NH_4^+,av}], [N_{NO_3^-,av}]$	PV	concentration of available N in DOM, ammonium-N, nitrate-N pools	kg/m^3
N_{LF}, N_{LS}, N_{SS}	PV	fast litter, slow litter, slow soil N contents	kg/m^2
$N_{NH_4^+}, N_{NO_3^-}$	PV	soil ammonium-N, nitrate-N contents	kg/m^2
S	PV	soil water content	unitless
T	PV	soil temperature	°C
River Equations			
$C_{NO_3^-}$	PV	nitrate-N concentration	µmol N/l
f_T'	PV	stream temperature reduction function	unitless
$F_{DON}^{in}, F_{NH_4^+}^{in}, F_{NO_3^-}^{in}$	DV	river inflow of DON, ammonium-N, nitrate-N	kg/m^2 s

$F_{DON}^{out}, F_{NH_4^+}^{out}, F_{NO_3^-}^{out}$	DV	river outflow of the DON, ammonium-N, nitrate-N	$kg/m^2\ s$
H	IF	river depth	m
k'_{denitr}	PV	reaction rate constant for river denitrification	$1/s$
$P_{DON}, P_{NH_4^+}, P_{NO_3^-}$	IF	point sources of DIN, ammonium-N, nitrate-N	$kg/m^2\ s$
$R_{DON}, R_{NH_4^+}, R_{NO_3^-}$	DV	DON, ammonium-N, nitrate-N in rivers	kg/m^2
T'	PV	water temperature	$°C$

Table 3. Susquehanna River Basin Geographic Statistics for the USGS and SRBC nutrient monitoring sites (McGonigal, 2011; USGS, 2014).

Site Location	Waterbody	Sub basin Area, km^2	2000 Land Use Percentages					
			Water/ Wetland	Urban	Agricultural		Forest	Other
					Cropland	Pasture		
7 Long-term Sites								
Towanda, 1989~	Susquehanna	20,194	2	5	17	5	71	0
Danville, 1985~	Susquehanna	29,060	2	6	16	5	70	1
Lewisburg, 1985~	W B Susque	17,734	1	5	8	2	84	0
Newport, 1985~	Juniata	8,687	1	6	14	4	74	1
Marietta, 1987~	Susquehanna	67,314	2	7	14	5	72	0
Conestoga, 1985~	Conestoga	1,217	1	24	12	36	26	1
Conowingo, 1985~	Susquehanna	70,189	2	9	7	19	63	0
9 Newly Introduced Sites								
Conklin, 2005~	Susquehanna	5,778	3	3	18	4	71	1
Smithboro, 2004~	Susquehanna	11,989	3	5	17	5	70	0
Campbell, 2005~	Cohocton	1,217	3	4	13	6	74	0
Chemung, 2004~	Chemung	6,488	2	5	15	5	73	0
Wilkes-Barre, 2004~	Susquehanna	25,785	2	6	16	5	71	0
Karthaus, 2004~	W B Susque	3,785	1	6	11	1	80	1
Castanea, 2004~	Bald Eagle	1,087	1	8	11	3	76	1
Saxton, 2004~	Raystown B Juni	1,957	<0.5	6	18	5	71	0
Manchester, 2004~	W Conewago	1,320	2	13	12	36	36	1

Table 4. Sub-basin area, 20 year (1986-2005) average applied non-point and point N sources, and simulated soil water content, temperature, nitrate-N content, and denitrification rate (% of the non-point N sources) for each of 6 sub-basins.

6 Sub-basins	Basin Area, km^2	Non-point N Sources kg/km^2 yr	Point N Sources kg/km^2 yr	Soil Water Content	Soil Temp. C	Soil Nitr. N kg/km^2	Soil Denitr. kg/km^2 yr
Upper Susquehanna	14,126	3,315	40	0.439	8.65	12,713	1,213 (37%)
Chemung	6,731	2,962	76	0.454	8.60	9,888	916 (31%)
Middle Susquehanna	9,847	3165	331	0.459	9.39	11,599	1,142 (36%)
West Branch Susquehanna	18,447	3,163	70	0.458	9.24	11,746	959 (30%)
Juniata	8,686	4,553	41	0.480	10.58	17,002	1,538 (34%)
Lower Susquehanna	16,070	6,098	163	0.463	10.27	27,358	2,717 (45%)

Table 5. Temporal evaluation of the annual stream discharges and N loads for the period 1987-2005 at Marietta. If a p-value is smaller than 0.05, the correlation between the modeled and reported data is significantly different from zero.

		Discharge	DN	Nit. N	Amm. N	DON
R^2		0.6	0.5	0.4	0.5	0.4
Corr. Coef.	Pearson's linear (p-value)	0.7 (< 0.0001)	0.7 (< 0.0001)	0.6 (0.0044)	0.7 (< 0.0001)	0.6 (0.0064)
	Spearman's rho (p-value)	0.7 (0.0011)	0.7 (< 0.0001)	0.6 (0.0056)	0.6 (0.0099)	0.6 (0.0160)

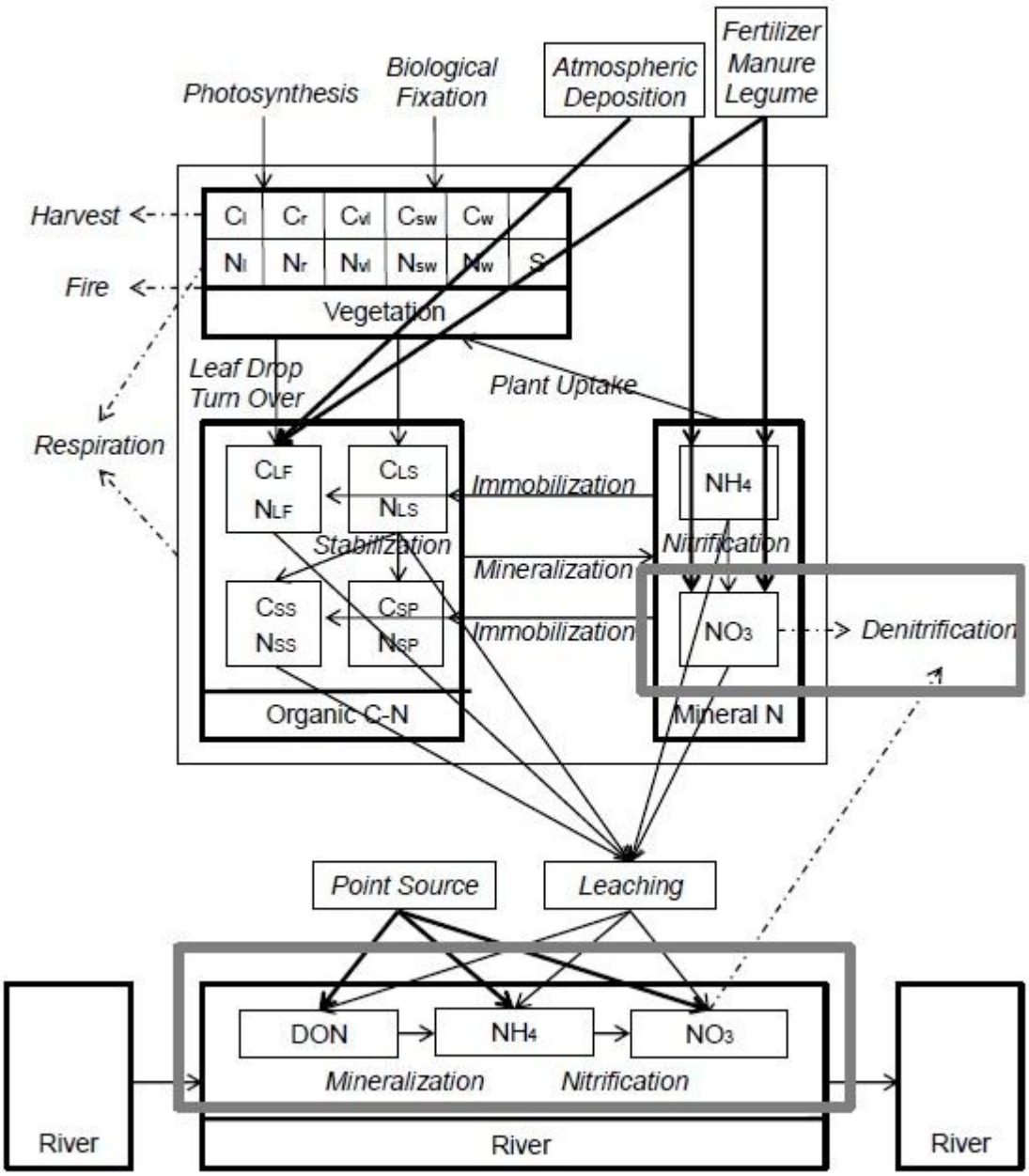

Figure 1. Structure of LM3-TAN. Two thick boxes show the incorporated denitrification module in the terrestrial component and stream microbial processes in the river component. The river systems are a series of continuously stirred tank reactors (CSTR) that simulate stream mineralization, nitrification, and denitrification. The other boxes show major C and N pools in vegetation (leaves, fine roots, labile, sapwood, heartwood, and N buffer storage), soil (fast and slow little, slow and passive soil, mineral N), and river (organic and mineral N). The arrows depict fluxes of anthropogenic N sources (thick solid), C-N organic compounds and

mineral N (thin solid) with associated processes (italic), and C and N lost to the atmosphere or anthropogenic pool (dashed).

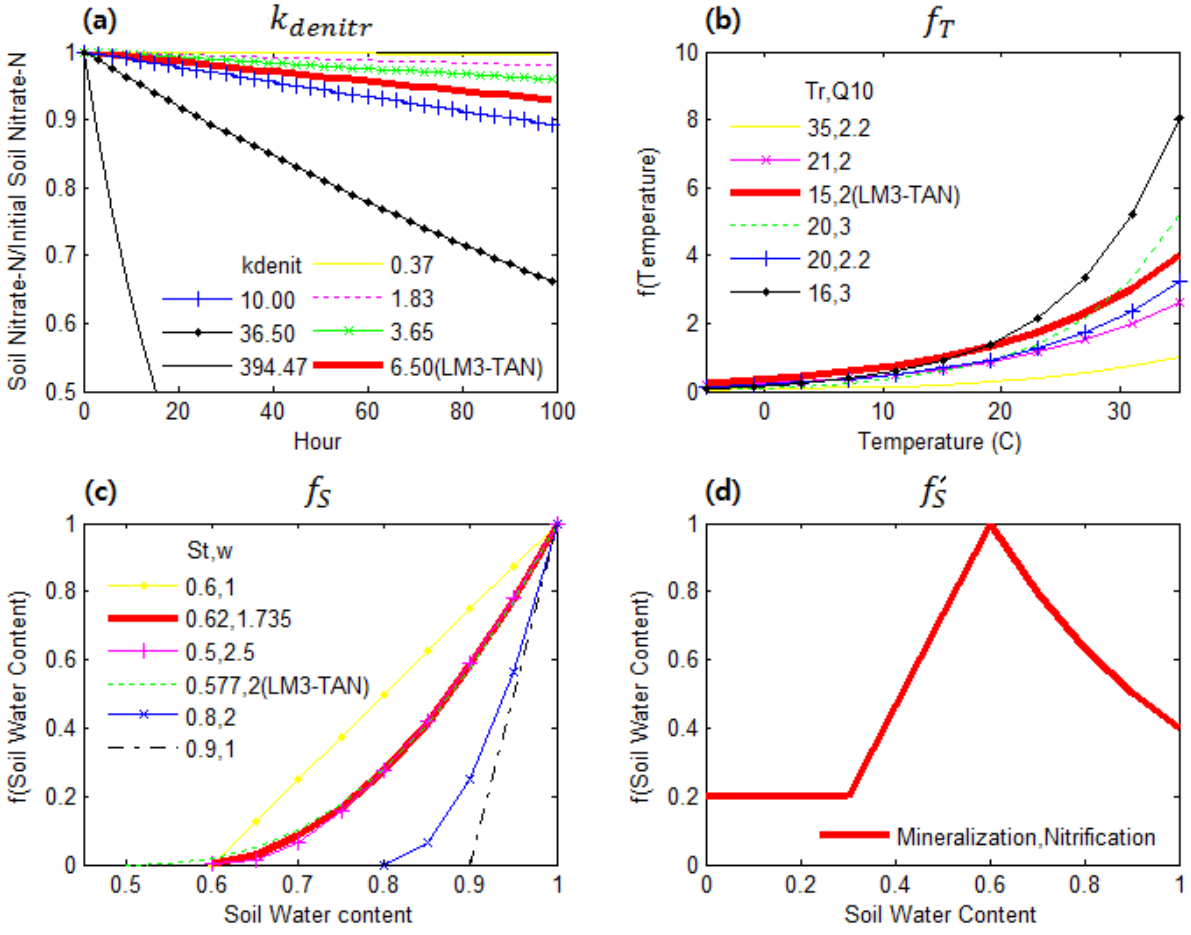

Figure 2. Overview of the denitrification module. Effects of first-order denitrification coefficient (a), soil temperature reduction function (b), soil water content reduction function (c) on soil denitrification rate; soil water content reduction function for mineralization and nitrification (d). The curves were produced using the Table 3, 6, and 7 in Heinen (2006).

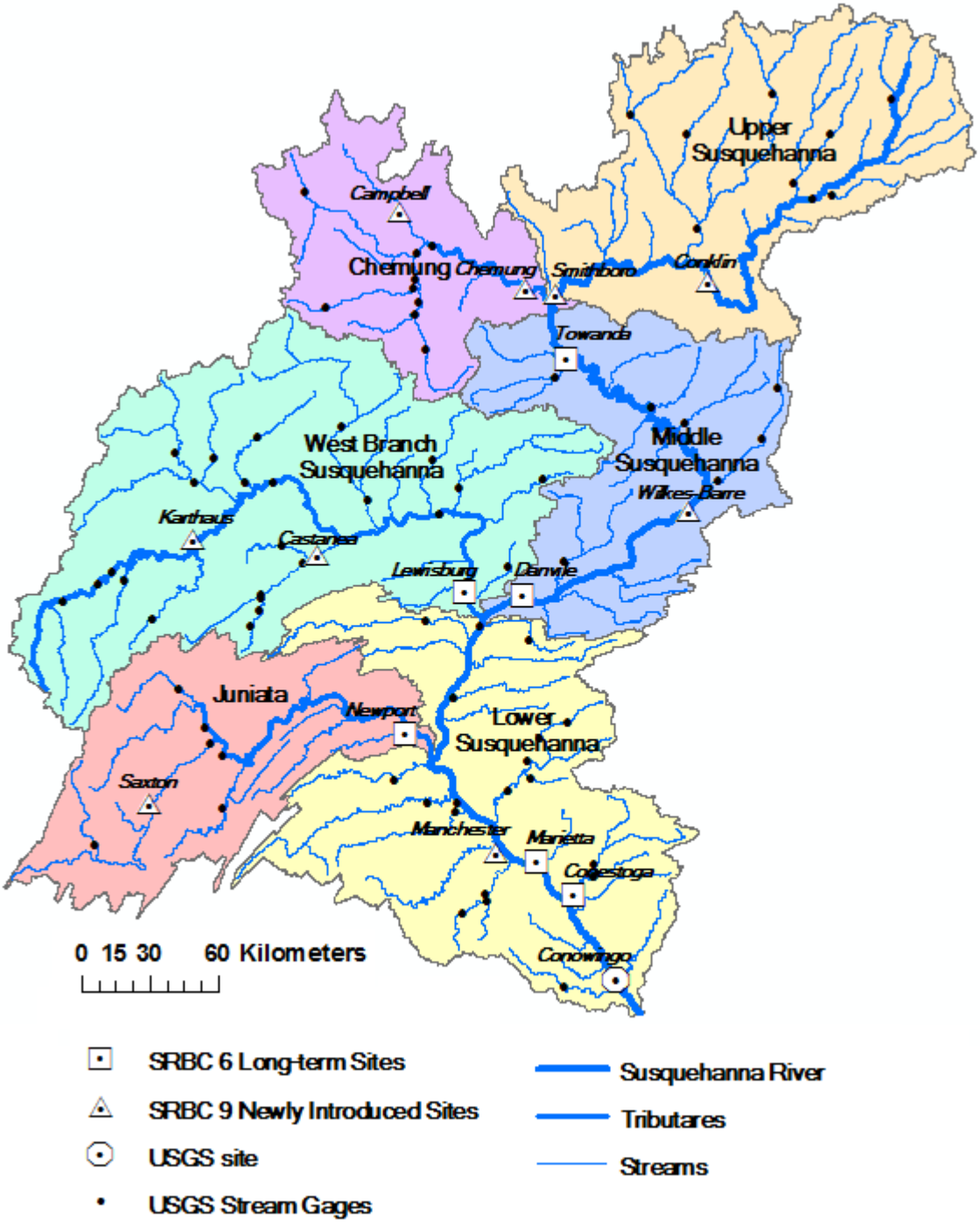

1

2

3 Figure 3. Map of the Susquehanna watershed, showing 6 major sub-basins, main stem of the
4 Susquehanna River, major tributaries (Chemung, West Branch Susquehanna, and Juniata
5 River), streams, and the location of USGS stream gauges and USGS and SRBC nutrient
6 monitoring sites.

7

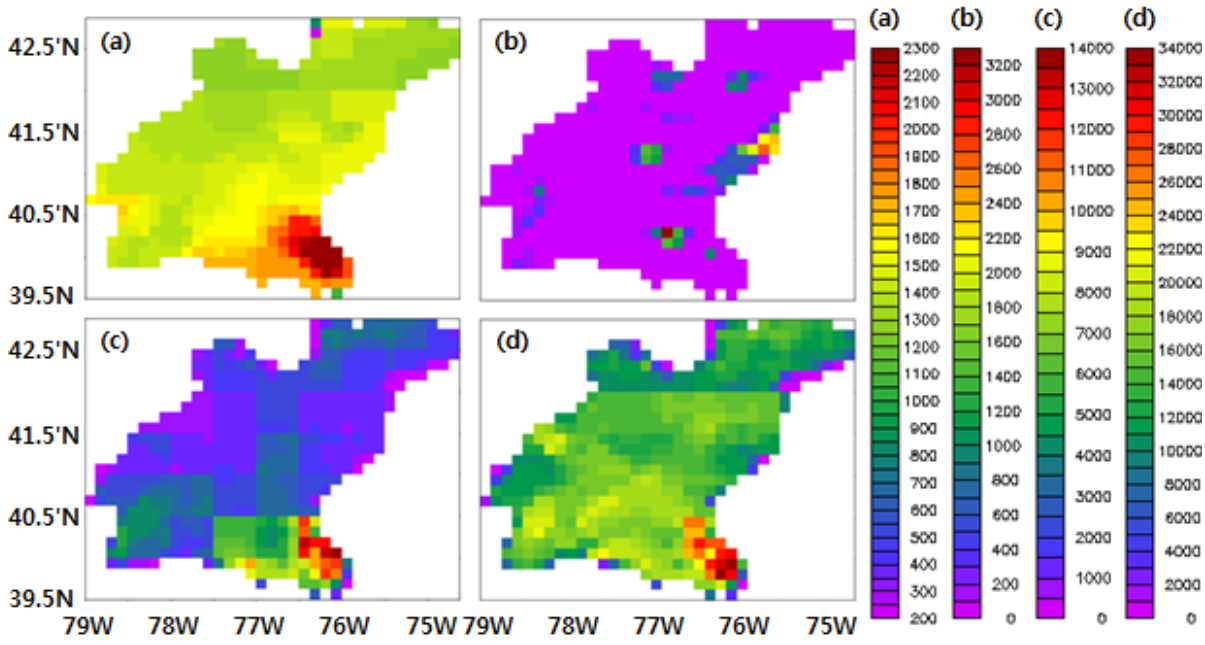

Figure 4. Spatial distribution maps of the applied 20 year (1986-2005) average anthropogenic N sources: atmospheric deposition (kg/km^2 year) (a), combined sewer overflow (kg/km^2 year) (b), and fertilizer, manure, and legume applications (kg/km^2 year) (c) and ($kg/crop\ land\ km^2$ year) (d).

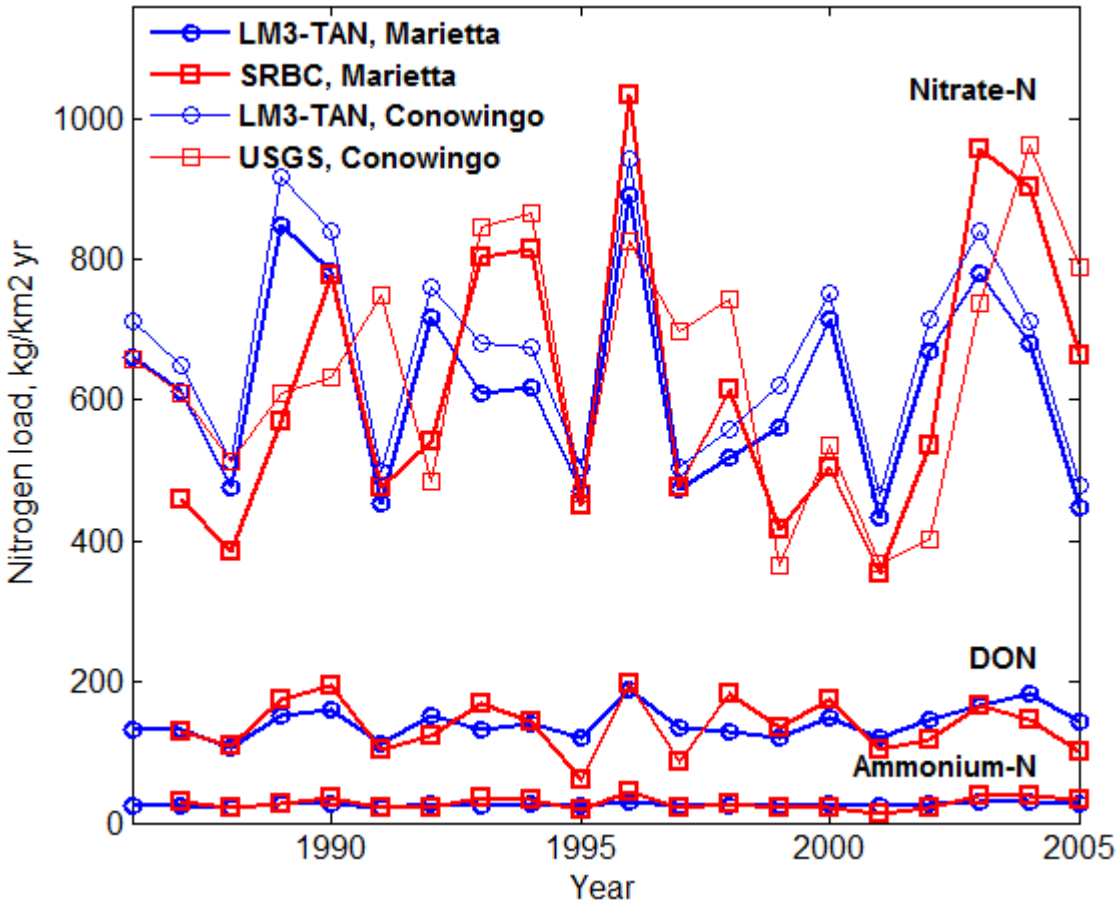

Figure 5. 20 years (1986-2005) of the simulated stream N loads (normalized by sub-basin areas) at Marietta and Conowingo and the corresponding reported data from SRBC and USGS.

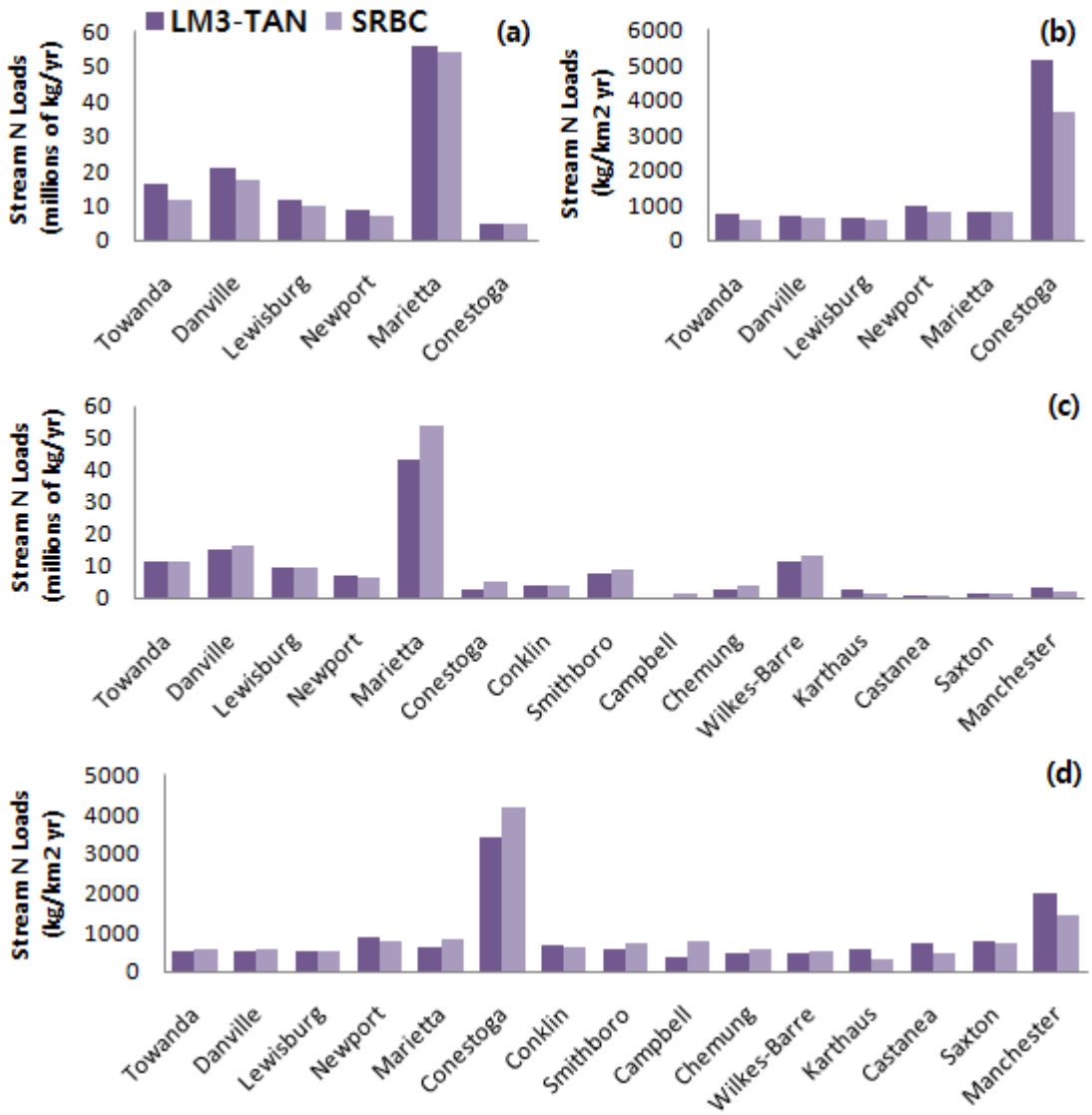

Figure 6. 17 year (1989-2005) average simulated and reported (SRBC) stream N loads at the 6 long-term monitoring sites in (a) millions of kg/yr and (b) kg/km^2 yr; simulated and reported stream N loads for the year 2005 at the 15 monitoring sites in (c) millions of kg/yr and (d) kg/km^2 yr.

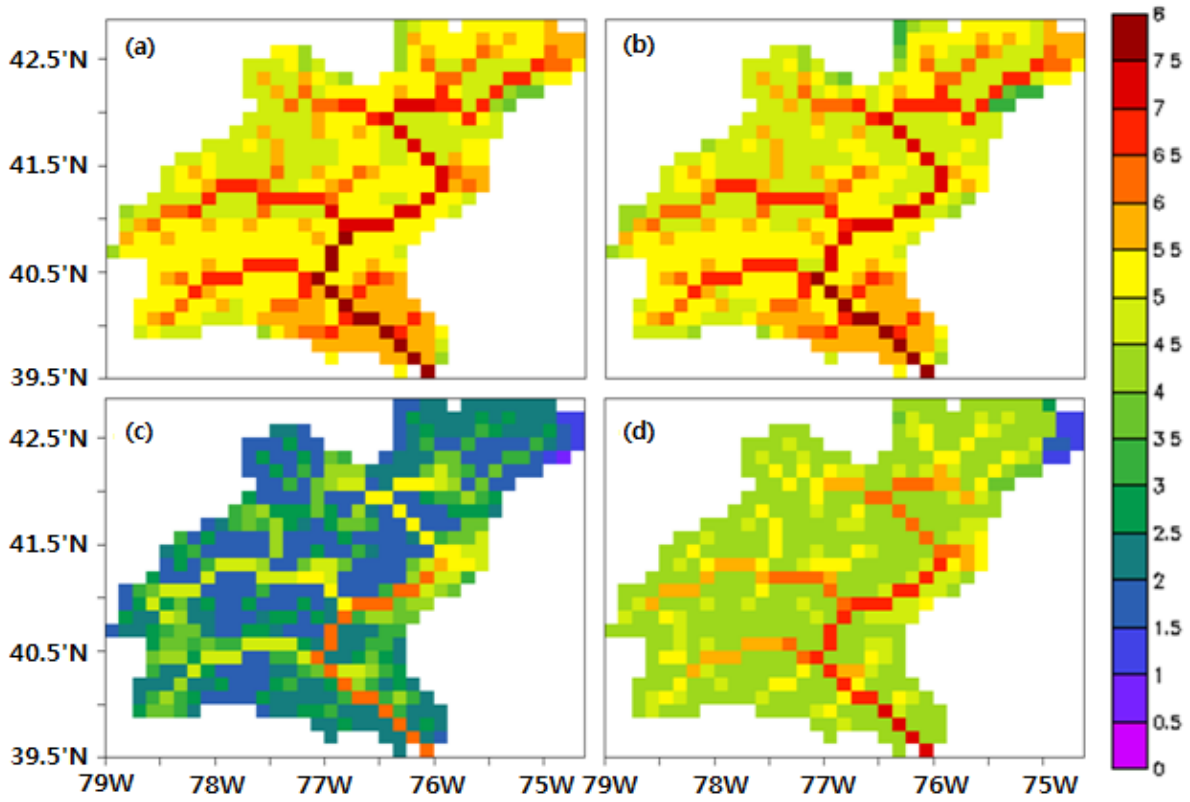

Figure 7. Spatial distribution maps of 20 year (1986-2005) average simulated stream (a) dissolved N, (b) nitrate N, (c) ammonium N, and (d) dissolved organic N loads, log (kg/year).

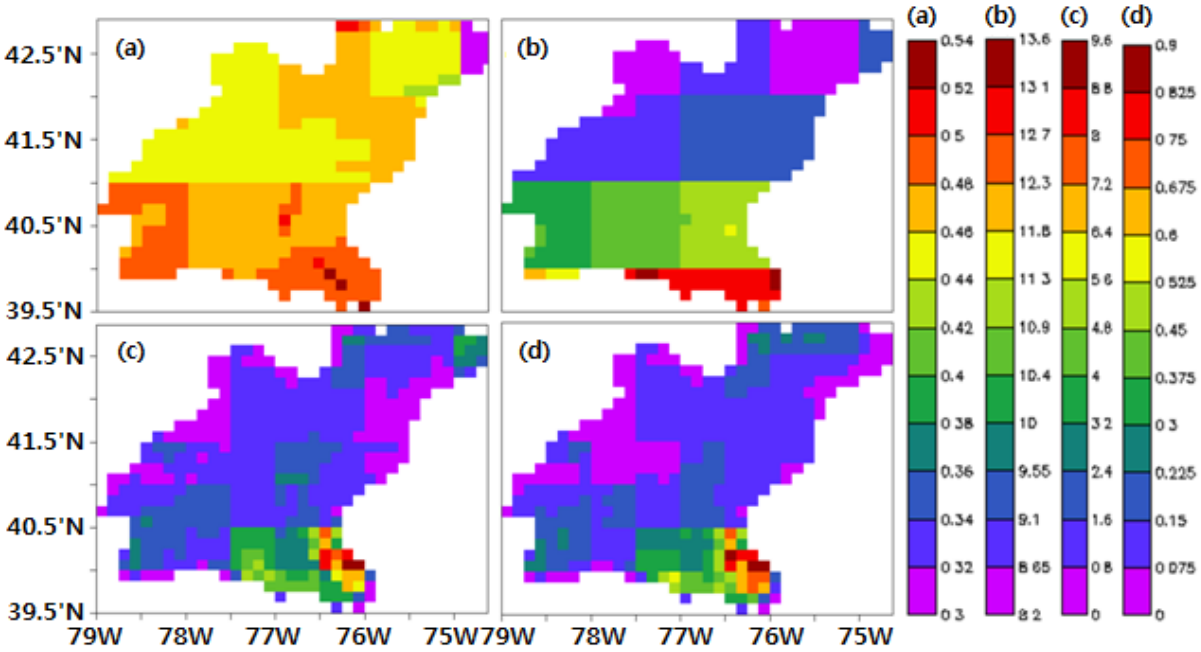

Figure 8. Spatial distribution maps of 20 year average (1986-2005) (a) soil water content, (b) temperature (℃), (c) nitrate N content ($10^2 \times \mathrm{kg/m^2\ year}$), and (d) denitrification rate ($10^2 \times \mathrm{kg/m^2\ year}$).

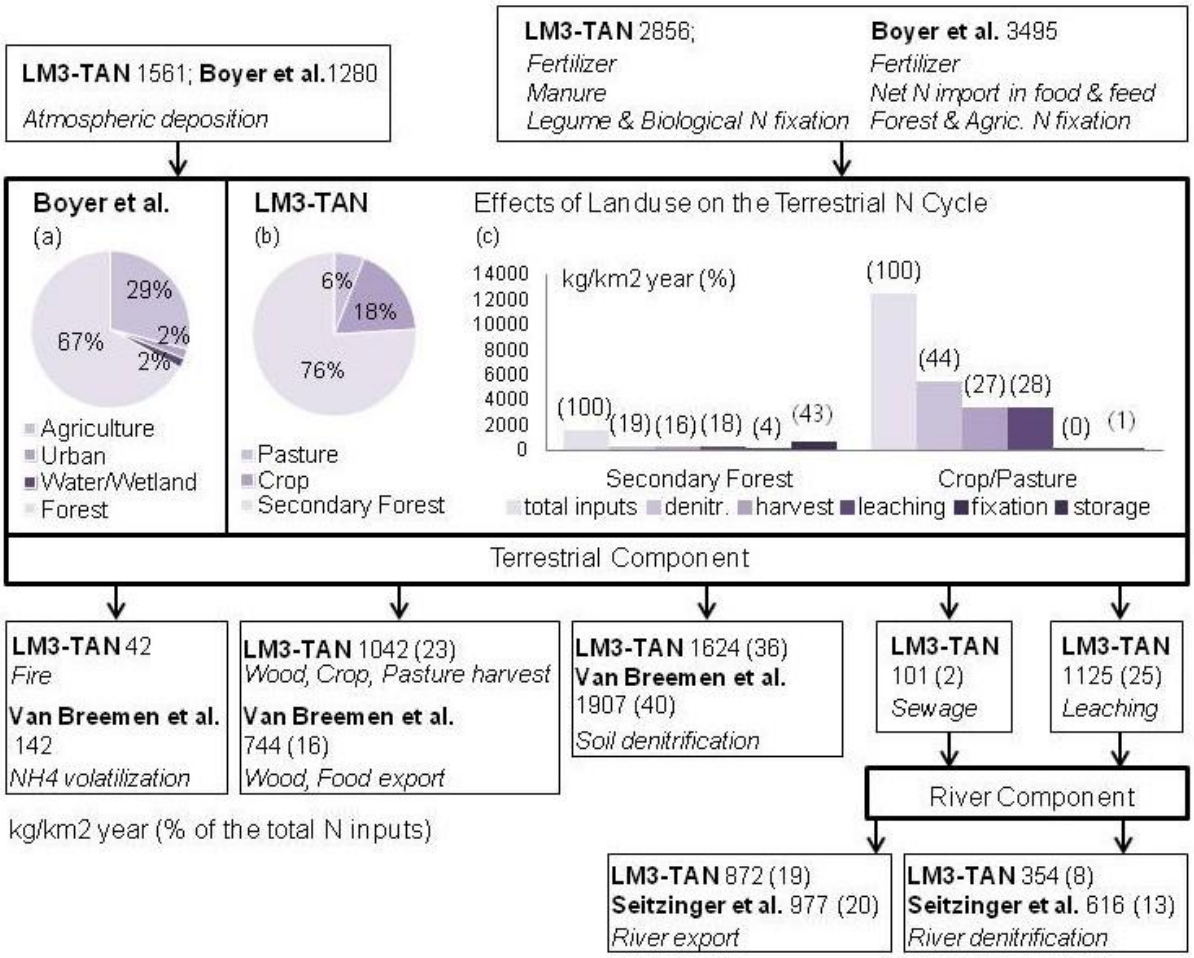

Figure 9. Comparison between the calculated and reported budgets of N sources, retention, lost, transport, and river export at the level of the whole Susquehanna watershed for the period 1988 to 1992 (Boyer et al., 2002; Breemen et al., 2002; Seitzinger et al., 2002; USEPA, 2010a).

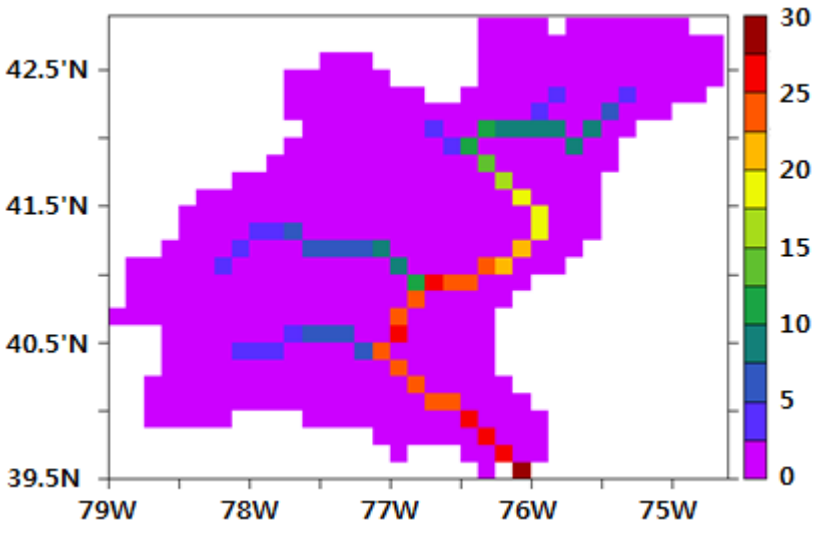

Figure 10. N removal by river denitrificaiton (%) = (river N load with "$k_{denitr}^{'}$=0"– river N load with "estimated $k_{denitr}^{'}$") / river N load with "$k_{denitr}^{'}$=0"× 100.